THE JOURNAL OF PHYSICAL CHEMISTRY Letters

Letter

pubs.acs.org/JPCL

Solute−Solvent Interactions and Excited-State Symmetry Breaking: Beyond the Dipole−Dipole and the Hydrogen-Bond Interactions

Bogdan Dereka and Eric Vauthey*

Department of Physical Chemistry, University of Geneva, 30 quai Ernest-Ansermet, CH-1211 Geneva 4, Switzerland

Supporting Information

ABSTRACT: Symmetry breaking of the excited state of a linear quadrupolar acceptor−donor−acceptor molecule was investigated using time-resolved infrared spectroscopy in 55 solvents allowing the influence of several solute−solvent interactions to be examined separately. No symmetry breaking was found in nonpolar solvents irrespective of their refractive index, indicating that differences in dispersion interactions between the two arms of the molecule do not suffice to induce an asymmetric distribution of the excitation. However, symmetry breaking was observed in nondipolar but quadrupolar solvents like benzene to an extent that can be as large as that found in medium dipolar solvents like THF. Whereas larger symmetry breaking occurs in the most dipolar solvents, the strongest are observed in protic solvents due to hydrogen bonding. Strong evidence of the formation of halogen bonds in the excited state is also presented, confirming the idea of symmetry-breaking-induced asymmetrical photochemistry.

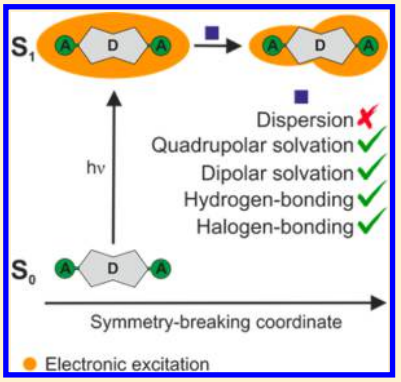

Over the past few years, there has been considerable activity in the synthesis and study of linear quadrupolar molecules with D−(π−A)$_2$ or A−(π-D)$_2$ motives, where D and A are electron-donating and -accepting groups, respectively. Such systems are predicted to have a large two-photon absorption cross section,[1−4] a most wanted property for numerous applications.[5−16] Although these molecules are centrosymmetric, it has been found that the lowest singlet excited state of most of them is highly dipolar, indicative of an asymmetric distribution of the electronic excitation on the two branches.[17−25] This excited-state symmetry breaking (SB) was suggested theoretically to be triggered by fluctuations of the structure and/or of the local field generated by the surrounding solvent.[26−30] Direct visualization of excited-state SB dynamics was recently achieved using time-resolved infrared (TRIR) spectroscopy by probing local vibrational modes localized in the two arms of the molecules.[31−33] For both molecules investigated, SB was only observed in dipolar solvents and was found to occur on similar timescales as those of solvent fluctuations. Hydrogen-bond interactions were also found to amplify the extent of SB initially originating from dipolar interactions.[32]

Here we report on a comprehensive study of the effect of solute−solvent interactions on excited-state SB of the D−(π−A)$_2$ molecule **1** (Scheme 1)[34,35] in 55 different solvents (Tables S1−S5), allowing additionally the effect of dispersion, quadrupolar, and halogen-bond interactions to be investigated. We present the first evidence, to the best of our knowledge, of a halogen bond in the excited state in liquid solution.

SB was monitored by looking at the −C≡N stretching mode of **1** in the excited state.[32] When purely quadrupolar, **1** is characterized by a single excited-state absorption band (ESA1) associated with the antisymmetric −C≡N stretching mode

Scheme 1. Principle of the Experiment[a]

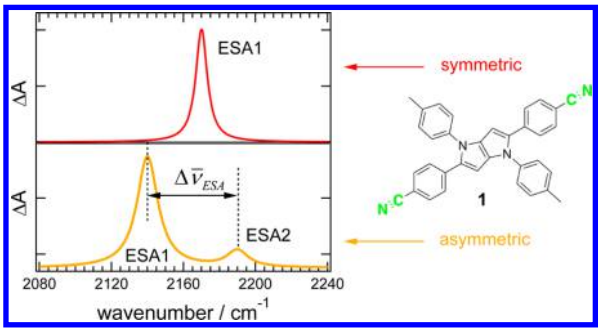

[a]When the excited state of **1** is symmetric, the transient IR spectrum in the −C≡N stretching region exhibits a single excited-state absorption band (ESA1). Upon SB, the spectrum shows two bands (ESA1 and ESA2).

(Scheme 1). As SB takes place, the symmetric −C≡N stretching mode is no longer IR-forbidden and appears in the TRIR spectrum as a second weaker band (ESA2). Moreover, the frequency splitting of these two bands, $\Delta\bar{\nu}_{ESA}$, as well as the ESA2/ESA1 intensity ratio, r_{ESA}, increases with SB.

The solvatochromism of the $S_1 \leftarrow S_0$ absorption band of **1** is dominated by dispersion interactions, as testified by the linear dependence of the transition energy on the solvent polarizability expressed as $f(n^2) = 2(n^2 - 1)/(2n^2 + 1)$ (Figure S1). The effect of dispersion on the excited-state SB was investigated by measuring the TRIR spectra of **1** in 11 apolar solvents, that

Received: July 14, 2017
Accepted: August 8, 2017
Published: August 8, 2017

DOI: 10.1021/acs.jpclett.7b01821
J. Phys. Chem. Lett. 2017, 8, 3927−3932

is, alkanes, cyclohexene, and CCl_4, which do not possess an electric dipole or polar bonds that could result in a significant quadrupolar moment and which allow $f(n^2)$ to be varied between 0.35 and 0.43 (Table S1). The TRIR spectra in all 11 solvents in the −C≡N stretching region show a single positive −C≡N band, ESA1, at around 2170 cm^{-1}, together with a very weak negative ground-state bleach at ∼2230 cm^{-1} (Figure 1a).

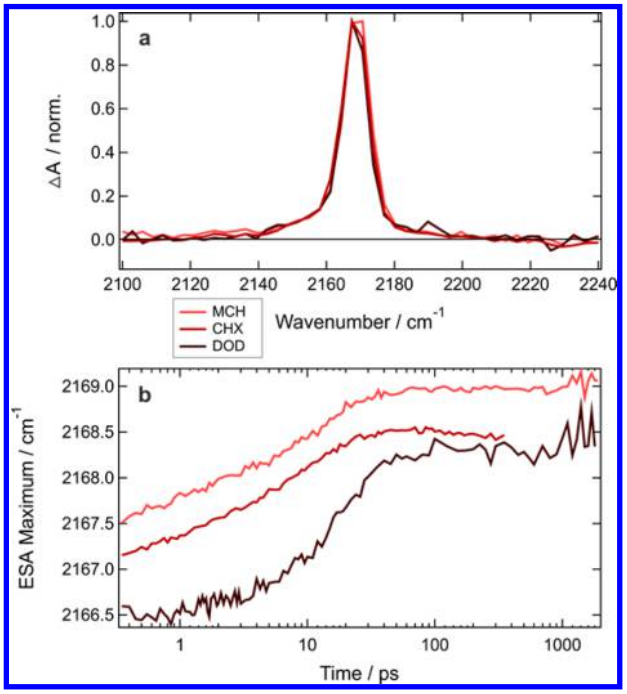

Figure 1. (a) TRIR spectra measured 100 ps after 400 nm excitation of **1** in apolar solvents. (b) Time dependence of the maximum of ESA1 in methylcyclohexane (MCH), cyclohexane (CHX), and dodecane (DOD) obtained from lineshape analysis.

The presence of a single excited-state band is an unambiguous indication that the S_1 state of **1** remains symmetric and purely quadrupolar during its whole lifetime. ESA1 exhibits a 1−2 cm^{-1} frequency upshift during the first few tens of picoseconds that can be ascribed to vibrational cooling (Figure 1b).[36−38] The magnitude of this upshift, obtained from a bandshape analysis of ESA1, increases slightly with $f(n^2)$ (Figure S2). This can be explained by the solvatochromism of the $S_1 \leftarrow S_0$ absorption band, that is, by an increasing amount of excess energy upon 400 nm excitation with increasing $f(n^2)$. The position of ESA1 in alkanes, once vibrational relaxation is completed, varies by less than 2 cm^{-1} (Figure S3). However, in cyclohexene and CCl_4, ESA1 it is downshifted respectively by 4 and 8 cm^{-1} relative to the alkanes, indicating that other interactions than dispersion might be operative in these two solvents.

In any case, these results show that neither structural fluctuations nor dispersion interactions are sufficient to break the symmetry of the excited state of **1**.

TRIR spectra of **1** were then recorded in a series of 11 nondipolar solvents containing dipolar bonds and conjugated π-systems, such as tetrachloroethylene, toluene, benzene, and fluorobenzenes (Table S2). These solvents have no dipole moment but are characterized by polar bonds and a quadrupolar moment. Maroncelli and coworkers showed that the fluorescence of the dipolar coumarin 153 in these solvents exhibits a substantial solvatochromism that correlates well with the effective quadrupole moment $\langle Q \rangle$.[39] In all 11 quadrupolar solvents, the TRIR spectra consist of two bands, the intense ESA1 and the weaker frequency-upshifted ESA2 testifying that SB is taking place (Figure 2a). Both bands are already observed at the earliest time delay, that is, at around 200 fs. However, $\Delta\bar{\nu}_{ESA}$, which reflects the extent of SB, increases within the first 10 ps after excitation, as testified by the red shift of ESA1 shown in Figure 2b. This temporal behavior is very similar to that observed in dipolar solvents.[32] The presence of both bands at early time indicates that the initial asymmetry of the solvent field and/or ultrafast inertial solvent motion are sufficient to break the symmetry of the excited state. However, further SB occurs as the quadrupolar solvent molecules reorient via diffusive motion. Because solvent relaxation and hence SB occur slightly faster than vibrational cooling in most solvents, the band maximum exhibits a U-shaped time evolution (Figure 2b). Although the dynamics associated with these processes cannot be determined precisely because of their temporal overlap, SB occurs on a similar time scale as the relaxation of these solvents.[39] Figure 2c reveals that the band splitting measured at long time delay, once the spectral dynamics is complete, increases with $\langle Q \rangle$. Given that $\langle Q \rangle$ is not easily accessible experimentally,[40] it was calculated as described in the SI (Table S2). The band splitting in CS_2 must be considered with caution because the S_1 state of **1** undergoes intersystem crossing to the triplet state in 25 ps (Figures S4 and S5), most probably as a consequence of an external heavy-atom effect. Therefore, the reported $\Delta\bar{\nu}_{ESA}$ does not correspond to a fully relaxed S_1 state.

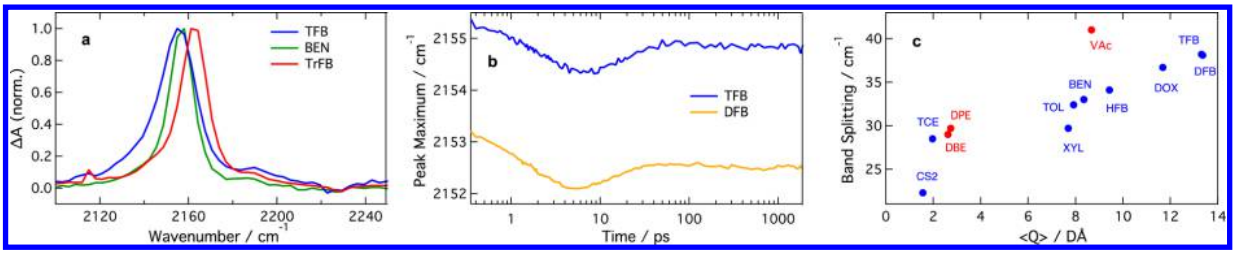

Figure 2. (a) TRIR spectra measured 100 ps after 400 nm excitation of **1** in quadrupolar solvents. (b) Time dependence of the ESA1 maximum in 1,3-di- and 1,2,4,5-tetra-fluorobenzene (DFB, TFB). The initial downshift reflects the increasing SB upon solvent relaxation, and hence an increasing $\Delta\bar{\nu}_{ESA}$, whereas the following upshift is due to vibrational cooling. (c) Splitting of ESA1 and ESA2, $\Delta\bar{\nu}_{ESA}$, as a function of the effective quadrupole moment, $\langle Q \rangle$. The red points designate three weakly dipolar solvents. (TrFB: 1,3,5-trifluorobenzene; TCE: tetrachloroethylene; XYL: xylene; TOL: toluene; BEN: benzene; HFB: perfluorobenzene; DOX: dioxane; TFB: 1,2,4,5-tetrafluorobenzene; DFB: 1,4-difluorobenzene; VAc: vinyl acetate; DPE: di-*n*-pentyl ether; DBE: di-*n*-butyl ether).

DOI: 10.1021/acs.jpclett.7b01821
J. Phys. Chem. Lett. 2017, 8, 3927−3932

Figure 2c suggests a linear relationship between the extent of SB and $\langle Q \rangle$. However, this linear correlation is most probably fortuitous because the positive intercept points to SB at $\langle Q \rangle$ = 0, in strong contradiction with the results in apolar solvents. A recent theoretical model of solvent-induced SB proposed by Ivanov et al.[41] that considers only dipole−dipole interactions predicts a nonlinear dependence of $\Delta\bar{\nu}_{ESA}$ on the Onsager polarity function $\Delta f = f(\varepsilon) - f(n^2)$, where ε is the dielectric constant, with a threshold below which the asymmetry of the solvent field around the solute is too small for SB to take place. The same can be expected here for the quadrupolar solvents. Consequently, the SB observed in the solvents with small $\langle Q \rangle$ most probably originates from other solute−solvent interactions or a combination of them, such as $\pi-\pi$ or octupolar interactions. It should also be noted that the TRIR spectra measured in the apolar solvents with the largest $f(n^2)$ value, namely, cyclohexene and CCl_4, and those with $\langle Q \rangle \leq \sim 4$ D·Å show a smooth transition from a single-band to double-band spectrum (Figure S6).

On the other hand, the correlation between the band splitting and the solvent quadrupole moment observed at $\langle Q \rangle >$ ~4 D·Å can be considered as genuine and reveals that SB takes place in solvents that are very often considered nonpolar because of their vanishingly small Δf value. The present results reveal that differences in dipole−quadrupole interactions between the two arms of **1** are sufficient to favor an asymmetric distribution of the excitation over the molecule and, thus, to enable SB. Therefore, nondipolar but quadrupolar solvents should be strictly distinguished from truly apolar solvents when investigating quadrupolar D−$(\pi$−A$)_2$ or A−$(\pi$−D$)_2$ molecules.

The effect of dipole−dipole interactions on the excited-state SB of **1** was already discussed.[32] Here, however, we report on 12 additional aprotic solvents including weakly polar ones with $\Delta f < 0.3$ ($\varepsilon < 4$), such as vinyl acetate (VAc) and several ethers (Table S3). SB is observed in all 18 dipolar solvents (Figure S7), with an extent, reflected by $\Delta\bar{\nu}_{ESA}$, that increases almost linearly with the Onsager polarity function above $\Delta f \approx 0.25$ (Figure 3). Below this value, $\Delta\bar{\nu}_{ESA}$ increases again as Δf tends to zero. The ESA2/ESA1 intensity ratio, r_{ESA}, which is another measure of the extent of SB, increases during the first ~10 ps (Figure S8). This temporal change reflects the increase of SB brought about by the diffusive motion of the polar solvent molecules. The final value of r_{ESA}, once this process is completed, correlates very well with $\Delta\bar{\nu}_{ESA}$ (Figure S9) and thus shows a similar dependence on Δf.

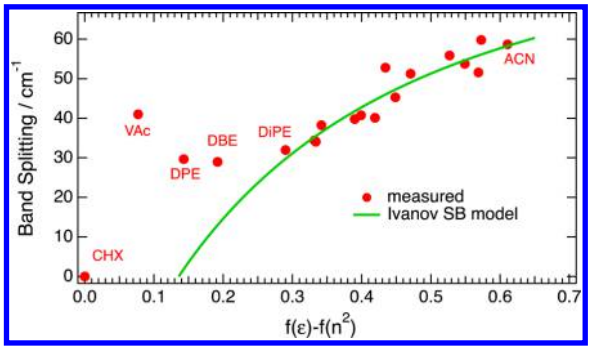

Figure 3. Band splitting, $\Delta\bar{\nu}_{ESA}$, vs the polarity function, $\Delta f = f(\varepsilon) - f(n^2)$. The continuous line is the splitting calculated according to the Ivanov SB model (see the SI for details. VAc: vinyl acetate; DPE: di-*n*-pentyl ether; DBE: di-*n*-butyl ether; DiPE: di-isopropyl ether; ACN: acetonitrile).

The correlation between the extent of SB and Δf observed at $\Delta f > 0.25$ can be well reproduced using the Ivanov SB model,[41] which only considers dipole−dipole interactions (see the SI for details). At $\Delta f < 0.25$, this model predicts a much smaller band splitting than that measured. Moreover, it points to a threshold value of $\Delta f = 0.14$ below which SB should not take place.

The three weakly dipolar solvents with $\Delta f < 0.25$ have a nonzero quadrupolar moment. The red points shown in Figure 2c represent the band splitting in these three solvents vs their effective quadrupolar moment. It appears that the contribution of the dipole−quadrupole interaction to the band splitting in VAc should be around 35 cm^{-1}, close to the value found experimentally. Similarly, SB in the weakly polar dipentyl- and dibutylethers most probably originates from the quadrupolar rather than the dipolar character of these solvents.

SB in protic solvents was already addressed earlier.[32] For the sake of comprehensiveness, we briefly summarize the main findings here. In these solvents, the first stages of SB originate from dipole−dipole interactions. After this initial SB, the two CN ends of **1** have a different basicity and, consequently, H-bond interactions are stronger with the more polar branch, that is, the branch with the highest density of excitation. This asymmetric H-bond interaction leads to further SB and to an increase of the band splitting with increasing H-bond-donating ability of the solvent, quantified by the Kamlet−Taft α parameter.[42] In "superprotic" solvents, with $\alpha >$ ~1.3, the interaction is strong enough to lead to a tight H-bond complex with a band splitting that is twice as large as that measured in the most polar aprotic solvents (Figure S10). This excited complex is also characterized by a substantially shorter lifetime than that in solvents with $\alpha < 1.3$ due to H-bond-induced nonradiative deactivation.[43]

This high sensitivity of the excited-state SB of **1** to hydrogen bonds prompted us to explore another specific but unorthodox interaction, namely, the halogen bond (X-bond) interaction, which is often considered as a hydrophobic analogue of the H-bond.[44−47] To the best of our knowledge, halogen bonding to an excited molecule has never been reported so far in liquid solution, but it was observed in the solid state where X-ray crystallography gives direct evidence of the short intermolecular distances. To test this, the excited-state dynamics of **1** was measured in perfluorinated isopropyl iodide (HFIP) and perfluorinated iodobenzene (IFB), two strong X-bond donors (Table S5).[48] Quantum-chemical calculations of the electrostatic potential surface of these two molecules confirm the presence of a large σ hole on the iodine atom (Figure S11).[49] This hole is larger and more positively charged with HFIP, indicating that this molecule is a stronger X-bond donor than IFB.

The excited-state lifetime of **1** in these two solvents is substantially reduced due to the occurrence of electron transfer (ET) to the solvent and amounts to 12 and 1.5 ps in IFB and HFIP, respectively. The slower ET in IFB allows for ISC via an external heavy-atom effect to be operative, and the T_1 state of **1** is observed after 20 ps (Figures S12 and S13). TRIR spectra measured directly after excitation of **1** in these two solvents are shown in Figure 4a. In IFB, ESA1 is significantly broader than that in aprotic solvents of similar polarity. Moreover, it undergoes an 8 cm^1 temporal downshift that is larger than that observed in any aprotic solvent ($\lesssim$4 cm^{-1}) but comparable to that in protic solvents with $0.8 < \alpha < 1.3$ (Figure 4b). This

DOI: 10.1021/acs.jpclett.7b01821
J. Phys. Chem. Lett. 2017, 8, 3927−3932

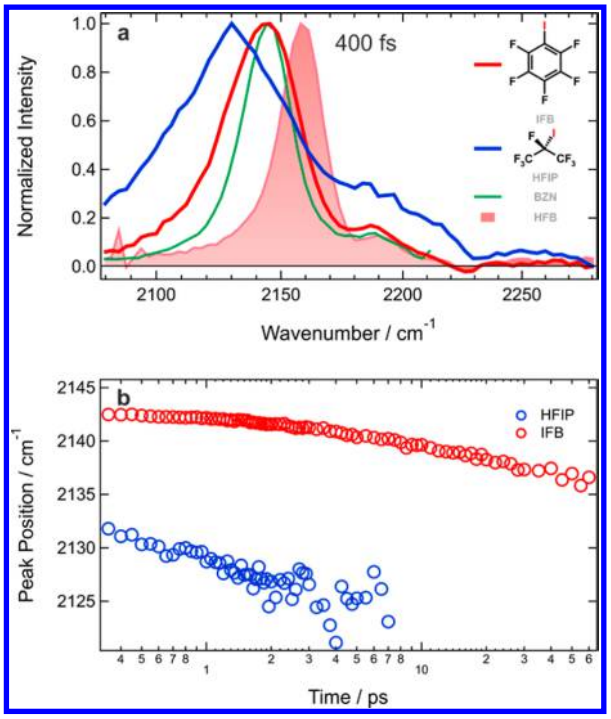

Figure 4. (a) TRIR spectra recorded directly after excitation of **1** in IFB and HFIP and in benzonitrile (BZN) and perfluorobenzene (HFB) for comparison. (b) Time dependence of the maximum of ESA1 in IFB and HFIP.

large temporal shift suggests SB via a specific interaction, that is, a halogen bond. This conclusion is supported by the TRIR measurements in HFIP, where the initial spectrum shows a significantly larger band splitting and intensity ratio, indicative of stronger SB (Figure 4a). Because of the occurrence of ET quenching, only the initial stage of the temporal shift of ESA1 is visible. However, Figure 4b suggests a larger shift than that in IFB, in agreement with larger SB.

All results in IFB and HFIP point to an additional solute–solvent interaction than those observed in the other solvents and suggest the occurrence of halogen bonding to **1** in the S_1 state. According to the position of the ground-state bleach in the TRIR spectra and the electronic absorption spectrum of **1** (Figure S14), this interaction is not significant in the ground state. Moreover, the temporal shift in the TRIR spectra, which can be explained by the relaxation of the halogen bond upon reorientation of the interacting and nearby solvent molecules, is observed with ESA1 only. This indicates that halogen bonding occurs only on the arm of **1**, which bears most of the excitation, and thus ESA2 is not significantly affected. Therefore, halogen bonding occurs only in the S_1 state after the initial SB due to dipolar interactions has taken place. This can be viewed as a SB-induced intermolecular photochemical process, confirming our idea of asymmetrical reactivity.[32]

The above results reveal the tremendous sensitivity of the excited-state SB in **1** to solute–solvent interactions. For this molecule, SB originates from differences in the orientation of the solvent molecules around its two arms. These differences are not large enough to result in a significant asymmetry of the dispersion interaction. Similarly, as **1** remains symmetric directly after excitation, it generates a symmetric electric field that in turns induces a symmetric reaction field in the polarizable solvent. Therefore, SB does not take place in these apolar solvents. However, these differences in orientation suffice for solvent molecules with quadrupolar character to generate a local field with enough asymmetry to induce SB. The amount of SB in the most quadrupolar solvents measured here is comparable to that found in a dipolar solvent like, for example, THF with Δf = ~0.4. Here, the band splitting amounts to ~40 cm^{-1}, whereas the largest $\Delta\bar{\nu}_{ESA}$ due to dipole–dipole interactions is around 60 cm^{-1}. Therefore, these quadrupolar solvents should imperatively not be considered as apolar. The quadrupolar character of nondipolar solvents is usually ignored in photoinduced charge-transfer studies, and solvents like benzene or toluene are often considered as nonpolar. Given the results reported here, the effect of the quadrupolar character of the solvent on these charge-transfer processes deserves attention.

Specific interactions lead to amplification of the SB because one of the two CN ends has a higher ability than the other to act as hydrogen and halogen bond acceptors. H-bond interactions can increase $\Delta\bar{\nu}_{ESA}$ beyond 100 cm^{-1}, whereas a halogen bond, observed here for the first time, leads to $\Delta\bar{\nu}_{ESA} \geq$ 80 cm^{-1}. Other specific interactions, such as π stacking, might also contribute to SB. The possible role of these interactions is worth further studies.

■ ASSOCIATED CONTENT

Supporting Information

The Supporting Information is available free of charge on the ACS Publications website at DOI: 10.1021/acs.jpclett.7b01821.

Tables with the properties of all 55 solvents, calculation of the effective quadrupole moment, experimental methods, absorption solvatochromism, additional transient IR absorption data, transient electronic absorption data, electrostatic potential surfaces of IFB and HFIP, and calculation of frequency splitting according to the Ivanov SB model (PDF)

■ AUTHOR INFORMATION

Corresponding Author

*E-mail: eric.vauthey@unige.ch.

ORCID

Bogdan Dereka: 0000-0003-2895-7915

Eric Vauthey: 0000-0002-9580-9683

Notes

The authors declare no competing financial interest.

■ ACKNOWLEDGMENTS

We wish to thank Prof. D. Gryko (Institute of Organic Chemistry of the Polish Academy of Sciences, Warsaw) for providing us with compound **1**. This work was supported by the Fonds National Suisse de la Recherche Scientifique through Project Nr. 200020-165890 and the University of Geneva.

■ REFERENCES

(1) Albota, M.; Beljonne, D.; Brédas, J. L.; Ehrlich, J. E.; Fu, J.-Y.; Heikal, A. A.; Hess, S. E.; Kogej, T.; Levin, M. D.; Marder, S. R.; et al. Design of Organic Molecules with Large Two-Photon Absorption Cross Sections. *Science* **1998**, *281*, 1653–1656.

(2) Brédas, J.-L.; Cornil, J.; Beljonne, D.; dos Santos, D. A.; Shuai, Z. Excited-State Electronic Structure of Conjugated Oligomers and Polymers: A Quantum-Chemical Approach to Optical Phenomena. *Acc. Chem. Res.* **1999**, *32*, 267–276.

(3) Rumi, M.; Ehrlich, J. E.; Heikal, A. A.; Perry, J. W.; Barlow, S.; Hu, Z.; McCord-Maughon, D.; Parker, T. C.; Röckel, H.;

DOI: 10.1021/acs.jpclett.7b01821
J. Phys. Chem. Lett. 2017, 8, 3927–3932

Thayumanavan, S.; et al. Structure−Property Relationships for Two-Photon Absorbing Chromophores: Bis-Donor Diphenylpolyene and Bis(styryl)benzene Derivatives. *J. Am. Chem. Soc.* **2000**, *122*, 9500−9510.
(4) Pawlicki, M.; Collins, H. A.; Denning, R. G.; Anderson, H. L. Two-Photon Absorption and the Design of Two-Photon Dyes. *Angew. Chem., Int. Ed.* **2009**, *48*, 3244−3266.
(5) Denk, W.; Strickler, J.; Webb, W. Two-Photon Laser Scanning Fluorescence Microscopy. *Science* **1990**, *248*, 73−76.
(6) Perry, J. W.; Ananthavel, S. P.; Barlow, S.; Dyer, D. L.; Ehrlich, J. E.; Erskine, L. L.; Heikal, A. a.; Kuebler, S. M.; Lee, I.-Y. S.; McCord-Maughon, D.; Cumpston, B. H.; et al. Two-Photon Polymerization Initiators for Three-Dimensional Optical Data Storage and Microfabrication. *Nature* **1999**, *398*, 51−54.
(7) Kawata, S.; Sun, H.-B.; Tanaka, T.; Takada, K. Finer Features for Functional Microdevices. *Nature* **2001**, *412*, 697−698.
(8) Tromayer, M.; Gruber, P.; Markovic, M.; Rosspeintner, A.; Vauthey, E.; Redl, H.; Ovsianikov, A.; Liska, R. A Biocompatible Macromolecular Two-Photon Initiator Based on Hyaluronan. *Polym. Chem.* **2017**, *8*, 451−460.
(9) Lee, K.-S.; Yang, D.-Y.; Park, S. H.; Kim, R. H. Recent Developments in the Use of Two-Photon Polymerization in Precise 2D and 3D Microfabrications. *Polym. Adv. Technol.* **2006**, *17*, 72−82.
(10) LaFratta, C. N.; Fourkas, J. T.; Baldacchini, T.; Farrer, R. A. Multiphoton Fabrication. *Angew. Chem., Int. Ed.* **2007**, *46*, 6238−6258.
(11) Walker, E.; Rentzepis, P. M. Two-Photon Technology: A New Dimension. *Nat. Photonics* **2008**, *2*, 406−408.
(12) Obata, K.; El-Tamer, A.; Koch, L.; Hinze, U.; Chichkov, B. N. High-Aspect 3D Two-Photon Polymerization Structuring with Widened Objective Working Range (WOW-2PP). *Light: Sci. Appl.* **2013**, *2*, e116.
(13) Gu, M.; Li, X.; Cao, Y. Optical Storage Arrays: a Perspective for Future Big Data Storage. *Light: Sci. Appl.* **2014**, *3*, e177.
(14) Helmchen, F.; Denk, W. Deep Tissue Two-Photon Microscopy. *Nat. Methods* **2005**, *2*, 932−940.
(15) Brown, S. B.; Brown, E. A.; Walker, I. The Present and Future Role of Photodynamic Therapy in Cancer Treatment. *Lancet Oncol.* **2004**, *5*, 497−508.
(16) Goodwin, A. P.; Mynar, J. L.; Ma, Y.; Fleming, G. R.; Fréchet, J. M. J. Synthetic Micelle Sensitive to IR Light via a Two-Photon Process. *J. Am. Chem. Soc.* **2005**, *127*, 9952−9953.
(17) Strehmel, B.; Sarker, A. M.; Detert, H. The Influence of σ and π Acceptors on Two-Photon Absorption and Solvatochromism of Dipolar and Quadrupolar Unsaturated Organic Compounds. *ChemPhysChem* **2003**, *4*, 249−259.
(18) Katan, C.; Terenziani, F.; Mongin, O.; Werts, M. H. V.; Porrès, L.; Pons, T.; Mertz, J.; Tretiak, S.; Blanchard-Desce, M. Effects of (Multi)branching of Dipolar Chromophores on Photophysical Properties and Two-Photon Absorption. *J. Phys. Chem. A* **2005**, *109*, 3024−3037.
(19) Woo, H. Y.; Liu, B.; Kohler, B.; Korystov, D.; Mikhailovsky, A.; Bazan, G. C. Solvent Effects on the Two-Photon Absorption of Distyrylbenzene Chromophores. *J. Am. Chem. Soc.* **2005**, *127*, 14721−14729.
(20) Amthor, S.; Lambert, C.; Dümmler, S.; Fischer, I.; Schelter, J. Excited Mixed-Valence States of Symmetrical Donor-Acceptor-Donor π Systems. *J. Phys. Chem. A* **2006**, *110*, 5204−5214.
(21) Carlotti, B.; Benassi, E.; Spalletti, A.; Fortuna, C. G.; Elisei, F.; Barone, V. Photoinduced Symmetry-Breaking Intramolecular Charge Transfer in a Quadrupolar Pyridinium Derivative. *Phys. Chem. Chem. Phys.* **2014**, *16*, 13984−13994.
(22) Kim, W.; Sung, J.; Grzybowski, M.; Gryko, D. T.; Kim, D. Modulation of Symmetry-Breaking Intramolecular Charge-Transfer Dynamics Assisted by Pendant Side Chains in π-Linkers in Quadrupolar Diketopyrrolopyrrole Derivatives. *J. Phys. Chem. Lett.* **2016**, *7*, 3060−3066.
(23) Dozova, N.; Ventelon, L.; Clermont, G.; Blanchard-Desce, M.; Plaza, P. Excited-State Symmetry Breaking of Linear Quadrupolar Chromophores: A Transient Absorption Study. *Chem. Phys. Lett.* **2016**, *664*, 56−62.
(24) Carlotti, B.; Benassi, E.; Fortuna, C. G.; Barone, V.; Spalletti, A.; Elisei, F. Efficient Excited-State Symmetry Breaking in a Cationic Quadrupolar System Bearing Diphenylamino Donors. *ChemPhysChem* **2016**, *17*, 136−146.
(25) Zhou, J.; Folster, C. P.; Surampudi, S. K.; Jimenez, D.; Klausen, R. S.; Bragg, A. E. Asymmetric Charge Separation and Recombination in Symmetrically Functionalized σ-π Hybrid Oligosilanes. *Dalton Trans.* **2017**, *46*, 8716−8726.
(26) Terenziani, F.; Painelli, A.; Katan, C.; Charlot, M.; Blanchard-Desce, M. Charge Instability in Quadrupolar Chromophores: Symmetry Breaking and Solvatochromism. *J. Am. Chem. Soc.* **2006**, *128*, 15742−15755.
(27) Sissa, C.; Parthasarathy, V.; Drouin-Kucma, D.; Werts, M. H. V.; Blanchard-Desce, M.; Terenziani, F. The Effectiveness of Essential-State Models in the Description of Optical Properties of Branched Push-Pull Chromophores. *Phys. Chem. Chem. Phys.* **2010**, *12*, 11715−11727.
(28) Terenziani, F.; Przhonska, O. V.; Webster, S.; Padilha, L. A.; Slominsky, Y. L.; Davydenko, I. G.; Gerasov, A. O.; Kovtun, Y. P.; Shandura, M. P.; Kachkovski, A. D.; et al. Essential-State Model for Polymethine Dyes: Symmetry Breaking and Optical Spectra. *J. Phys. Chem. Lett.* **2010**, *1*, 1800−1804.
(29) Rebane, A.; Drobizhev, M.; Makarov, N. S.; Wicks, G.; Wnuk, P.; Stepanenko, Y.; Haley, J. E.; Krein, D. M.; Fore, J. L.; Burke, A. R.; et al. Symmetry Breaking in Platinum Acetylide Chromophores Studied by Femtosecond Two-Photon Absorption Spectroscopy. *J. Phys. Chem. A* **2014**, *118*, 3749−3759.
(30) Vauthey, E. Photoinduced Symmetry-Breaking Charge Separation. *ChemPhysChem* **2012**, *13*, 2001−2011.
(31) Dereka, B.; Rosspeintner, A.; Li, Z.; Liska, R.; Vauthey, E. Direct Visualization of Excited-State Symmetry Breaking Using Ultrafast Time-Resolved Infrared Spectroscopy. *J. Am. Chem. Soc.* **2016**, *138*, 4643−4649.
(32) Dereka, B.; Rosspeintner, A.; Krzeszewski, M.; Gryko, D. T.; Vauthey, E. Symmetry-Breaking Charge Transfer and Hydrogen Bonding: Toward Asymmetrical Photochemistry. *Angew. Chem., Int. Ed.* **2016**, *55*, 15624−15628.
(33) Dereka, B.; Koch, M.; Vauthey, E. Looking at Photoinduced Charge Transfer Processes in the IR: Answers to Several Long-Standing Questions. *Acc. Chem. Res.* **2017**, *50*, 426−434.
(34) Janiga, A.; Glodkowska-Mrowka, E.; Stoklosa, T.; Gryko, D. T. Synthesis and Optical Properties of Tetraaryl-1,4-dihydropyrrolo[3,2-b]pyrroles. *Asian J. Org. Chem.* **2013**, *2*, 411−415.
(35) Krzeszewski, M.; Thorsted, B.; Brewer, J.; Gryko, D. T. Tetraaryl-, Pentaaryl-, and Hexaaryl-1,4-dihydropyrrolo[3,2-b]-pyrroles: Synthesis and Optical Properties. *J. Org. Chem.* **2014**, *79*, 3119−3128.
(36) Hamm, P.; Ohline, S. M.; Zinth, W. Vibrational Cooling after Ultrafast Photoisomerisation of Azobenzene Measured by fs Infrared Spectroscopy. *J. Chem. Phys.* **1997**, *106*, 519−529.
(37) Keane, P. M.; Wojdyla, M.; Doorley, G. W.; Watson, G. W.; Clark, I. P.; Greetham, G. M.; Parker, A. W.; Towrie, M.; Kelly, J. M.; Quinn, S. J. A Comparative Picosecond Transient Infrared Study of 1-Methylcytosine and 5′-dCMP That Sheds Further Light on the Excited States of Cytosine Derivatives. *J. Am. Chem. Soc.* **2011**, *133*, 4212−4215.
(38) Koch, M.; Rosspeintner, A.; Adamczyk, K.; Lang, B.; Dreyer, J.; Nibbering, E. T. J.; Vauthey, E. Real-Time Observation of the Formation of Excited Radical Ions in Bimolecular Photoinduced Charge Separation: Absence of the Marcus Inverted Region Explained. *J. Am. Chem. Soc.* **2013**, *135*, 9843−9848.
(39) Reynolds, L.; Gardecki, J. A.; Frankland, S. J. V.; Horng, M. L.; Maroncelli, M. Dipole Solvation in Nondipolar Solvents: Experimental Studies of Reorganization Energies and Solvation Dynamics. *J. Phys. Chem.* **1996**, *100*, 10337−10354.
(40) Buckingham, A. D. Molecular Quadrupole Moments. *Q. Rev., Chem. Soc.* **1959**, *13*, 183−214.

DOI: 10.1021/acs.jpclett.7b01821
J. Phys. Chem. Lett. 2017, 8, 3927−3932

(41) Ivanov, A. I.; Dereka, B.; Vauthey, E. A Simple Model of Solvent-Induced Symmetry-Breaking Charge Transfer in Excited Quadrupolar Molecules. *J. Chem. Phys.* **2017**, *146*, 164306.
(42) Taft, R. W.; Kamlet, M. J. The Solvatochromic Comparison Method. 2. The α-Scale of Solvent Hydrogen-Bond donor (HBD) Acidities. *J. Am. Chem. Soc.* **1976**, *98*, 2886−94.
(43) Dereka, B.; Vauthey, E. Direct Local Solvent Probing by Transient Infrared Spectroscopy Reveals the Mechanism of Hydrogen-Bond Induced Nonradiative Deactivation. *Chem. Sci.* **2017**, *8*, 5057−5066.
(44) Cavallo, G.; Metrangolo, P.; Milani, R.; Pilati, T.; Priimagi, A.; Resnati, G.; Terraneo, G. The Halogen Bond. *Chem. Rev.* **2016**, *116*, 2478−2601.
(45) Priimagi, A.; Cavallo, G.; Metrangolo, P.; Resnati, G. The Halogen Bond in the Design of Functional Supramolecular Materials: Recent Advances. *Acc. Chem. Res.* **2013**, *46*, 2686−2695.
(46) Politzer, P.; Murray, J. S.; Clark, T. Halogen Bonding: an Electrostatically-Driven Highly Directional Noncovalent Interaction. *Phys. Chem. Chem. Phys.* **2010**, *12*, 7748−7757.
(47) Riley, K. E.; Murray, J. S.; Fanfrlík, J.; Řezáč, J.; Solá, R. J.; Concha, M. C.; Ramos, F. M.; Politzer, P. Halogen Bond Tunability I: the Effects of Aromatic Fluorine Substitution on the Strengths of Halogen-Bonding Interactions Involving Chlorine, Bromine, and Iodine. *J. Mol. Model.* **2011**, *17*, 3309−3318.
(48) Hawthorne, B.; Fan-Hagenstein, H.; Wood, E.; Smith, J.; Hanks, T. Study of the Halogen Bonding between Pyridine and Perfluoroalkyl Iodide in Solution Phase Using the Combination of FTIR and 19F NMR. *Int. J. Spectrosc.* **2013**, *2013*, 1−10.
(49) Clark, T.; Hennemann, M.; Murray, J. S.; Politzer, P. Halogen Bonding: the σ-Hole. *J. Mol. Model.* **2007**, *13*, 291−296.

DOI: 10.1021/acs.jpclett.7b01821
J. Phys. Chem. Lett. 2017, 8, 3927−3932